

# CHARACTERIZING CONTACTS TO P-TYPE CdTe IN CdS/CdTe SOLAR CELLS

B. E. McCandless, J. E. Phillips and J. Titus  
Institute of Energy Conversion, University of Delaware, Newark, DE 19716 USA

**ABSTRACT:** Contacts to p-type CdTe in CdS/CdTe thin film polycrystalline solar cells made by physical vapor deposition were analyzed using current-voltage-temperature (J-V-T) and glancing-incidence x-ray diffraction measurements. The electrical properties of the CdTe/contact and those of the main CdS/CdTe junction were modeled with a series connected equivalent circuit consisting of a temperature independent resistance, a leaky diode representing the contact and a diode representing the main CdS/CdTe junction. The barrier heights of the CdS/CdTe junction diode and the CdTe contact diode were determined from J-V measurements made as a function of temperature. Barrier heights of 1.4 eV and 0.3 eV were found for the CdS/CdTe junction and the CdTe contact, respectively. The 0.3 eV barrier height of the CdTe contact junction is consistent with a CdTe/Cu<sub>x</sub>Te junction. The existence of a layer containing copper tellurides in working devices was confirmed by glancing incidence x-ray diffraction analysis of the CdTe surface prior to metallization.

**Keywords:** CdTe - 1: Thin Film - 2: Devices - 3

## 1. BACKGROUND

In superstrate CdTe-based thin film solar cells, the electrical behavior of the p-type CdTe contact depends upon the conductivity of the CdTe and the resulting band alignment between the CdTe and the contact material. The requirement of low contact resistance for optimal performance of the device means that the contact must provide a negligible barrier to majority carriers when operating at forward bias. In order to maintain a low resistance contact on superstrate CdS/CdTe devices, it is necessary to control the electrical conductivity of the CdTe layer and its exposed surface. In practice, this is achieved by controlling post-deposition processing parameters such as heat treatment and chemical surface modification [1,2]. The degree of post-deposition processing needed to attain the desired conductivity depends in part on the technique used to form the CdTe layer, but all cell making processes rely on formation of a p+ layer on the CdTe surface to form the primary contact to CdTe. Typically, Cu, excess Te, or a combination of these and other materials are used to facilitate contact formation. In earlier papers we described a contacting procedure that is applicable to CdTe made by several methods [2,3]. The resulting CdTe contact can exhibit various degrees of leaky diode "blocking" behavior under different conditions: 1) at room temperature if insufficient Cu is used; 2) at lower temperatures; and 3) after stressing devices at  $V_{oc}$  and  $T \sim 100^\circ\text{C}$  [4]. In stress-degraded devices, removing the current-carrying contact, re-etching the surface, and re-applying a contact removes the leaky diode "blocking" behavior. Thus, this behavior can be attributed to the CdTe/contact interface. To gain additional information about the nature of the CdTe contact surface, glancing incidence x-ray diffraction measurements were made. Making measurements at each processing stage directly revealed the chemical effect of each processing step.

## 2. EXPERIMENTAL

Thin film CdS/CdTe films were deposited by thermal evaporation from high purity CdS and CdTe source powders in a superstrate configuration onto ITO-coated Corning 7059 glass as indicated in Figure 1.

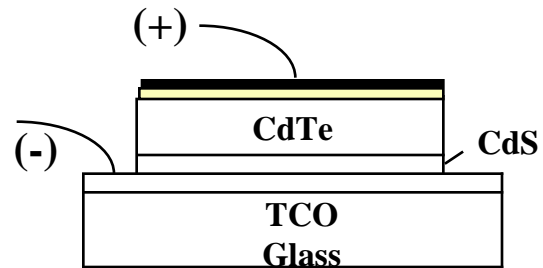


**Figure 1:** Cross-section schematic of CdS/CdTe solar cell. The gray band between the CdTe layer and the black current-carrying conductor represents the primary electrical contact to CdTe.

The CdS and CdTe thicknesses were  $0.18 \mu\text{m}$  and  $4$  to  $5 \mu\text{m}$ , respectively. Prior to contact processing, the structures were heat treated in a vapor mixture of  $\text{CdCl}_2$  and  $\text{O}_2$  [5]. The primary contact to the CdTe surface was prepared by a six-step wet chemical process (Table I).

At different stages of surface preparation, glancing incidence x-ray diffraction measurements were made at  $1^\circ$  incident beam angle with Cu-k x-rays to determine the chemical phase composition of the contact region. At glancing incident beam angles of  $\sim 1^\circ$ , the sampling depth is  $\sim 100 \text{ nm}$ .

**Table I.** Processing steps used after  $\text{CdCl}_2:\text{O}_2$  heat treatment to form primary contact to p-type CdTe.

Contact Process
Reaction in $\text{Br}_2:\text{CH}_3\text{OH}$
Reaction in aqueous $\text{K}_2\text{Cr}_2\text{O}_7:\text{H}_2\text{SO}_4$
Reaction in aqueous $\text{N}_2\text{H}_4$
Evaporation of 15 nm Cu
Vacuum heat treatment at $200^\circ\text{C}$
Reaction in $\text{Br}_2:\text{CH}_3\text{OH}$

Following the last bromine-methanol reaction, Acheson 505SS carbon ink conductor was applied to the surface, and the area of the devices were defined by mechanical scribing [2]. Current-voltage ( $J$ - $V$ ) measurements were made in the dark and under Xe arc lamp illumination. Measurements at different temperatures allowed determination of the barrier heights of the main CdS/CdTe junction and the primary CdTe contact.

### 3. J-V MEASUREMENTS AND ANALYSIS

The J-V behavior at various temperatures for a CdS/CdTe device made by physical vapor deposition with a carbon contact is shown in Figure 2. At room temperature and above the slopes ( $dV/dJ$ ) of the forward

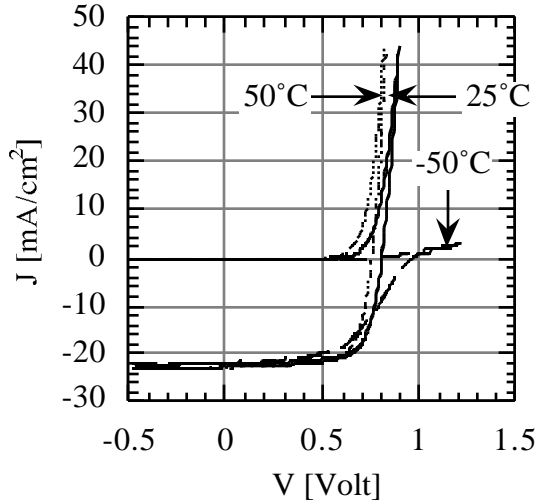


**Figure 2:**  $J$ - $V$  data of a CdS/CdTe device under AM1.5G illumination and dark showing the effect of the contact at various temperatures.

bias dark and light characteristics decrease monotonically with increasing voltage. At  $-50^\circ\text{C}$ , however, the dark and light forward bias  $J$ - $V$  characteristics exhibit an inflection point ("blocking" behavior) in forward bias. Similar "blocking" behavior has been obtained at room temperature after thermal and electrical stressing [4] and for devices made without copper in the contacting process [2]. Finally, we have found that for stress-degraded devices, the "blocking" behavior can be eliminated by removing the original

contact, re-etching the surface, and applying a new contact. All of this suggests the existence of a junction in the interface between CdTe and the current-carrying conductor whose properties depend critically on sample preparation and subsequent treatment.

The device is modeled with an equivalent circuit series connection of a temperature independent resistance ( $R_0$ ), a leaky diode representing the contact ( $J_C$ ) and a diode representing the main CdS/CdTe junction ( $J_J$ ) (Figure 3).

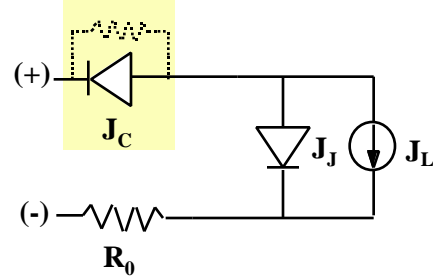


**Figure 3:** Equivalent circuit model with a temperature independent resistance ( $R_0$ ), a leaky diode representing the contact ( $J_C$ ) and a diode representing the main CdS/CdTe junction ( $J_J$ ).

The primary CdTe/contact is shown with a shunt path to account for non-zero slope at far forward bias. To model circuit behavior near the device  $V_{oc}$ , however, we only consider the two diodes, the lumped resistor, and the current generator. This model assumes that the two diodes are electrically separate and that the back diode operates only as a dark diode.

In forward bias, near  $V_{oc}$  of the main junction, the total series resistance of the device is the sum of contributions from the lumped resistor,  $R_0$ , and the primary contact,  $R_C$ :

$$R_S = R_0 + R_C, \quad (1)$$

where the  $R_C$  contribution is due to the contact diode:

$$R_C = \frac{V_C}{J_C}. \quad (2)$$

The forward current through the equivalent circuit is limited by the contact diode current,  $J_C$ , and can be represented as:

$$J = -J_{00c} e^{-\frac{c}{kT}} e^{\frac{qV_C}{A_c kT}} - 1, \quad (3)$$

where the prefactor,  $J_{00c}$ , and exponent,  $e^{-\frac{c}{kT}}$ , are the reverse saturation current of the contact diode,  $J_{0c}$ . For small voltage drops,  $qV_C/A_c kT \ll 1$ , Equation 3 reduces to:

$$J = \frac{qJ_{00c}}{A_c kT} e^{-\frac{c}{kT}} \quad (4)$$

Substituting into Equation 1 and solving for  $R_C$ :

$$R_C = R_S - R_0 \frac{A_c kT}{qJ_{00c}} e^{-\frac{c}{kT}} \quad (5)$$

The barrier height for the contact diode,  $F_C$ , was obtained from the Arrhenius slope,  $\ln(R_C)$  versus  $q/kT$ .  $R_S$  was evaluated from measurements of the device forward bias slope,  $dV/dJ$ , at elevated temperatures:

$$\frac{dV}{dJ} = R_S + \frac{(A_j kT)}{q(J + J_L)} \quad (6)$$

The temperature dependence of the dark forward bias slope,  $dV/dJ$ , is shown in Figure 4 for different measurement temperatures. At high temperature,  $R_C \sim 0$ , and  $R_S \sim R_0$ . Using the minimum  $R$  as  $R_0$  ( $0.3 \text{ } \Omega\text{-cm}^2$ ), the contact diode barrier height was determined using Equation 5 to be 0.33 eV (Figure 5).

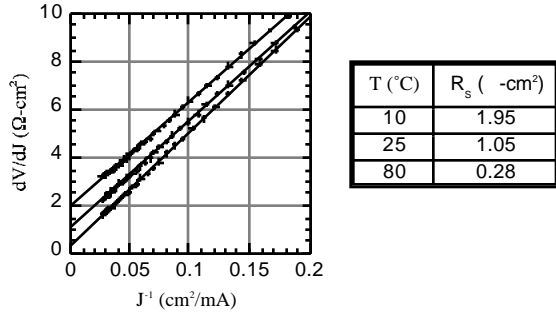


**Figure 4:**  $dV/dJ$  derived from dark J-V measurements for a CdS/CdTe device showing the temperature dependence of  $R_s$ . From this data, the minimum value of  $R_s$  ( $0.3 \text{ } \Omega\text{-cm}^2$ ) is taken as  $R_0$ .

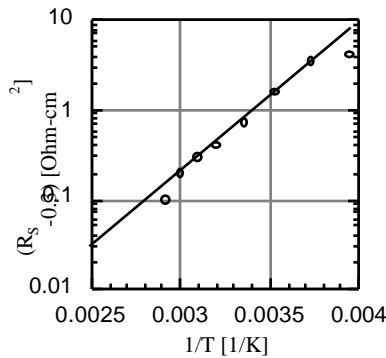


**Figure 5:** Temperature dependence of  $R_s$  with  $R_0 = 0.3 \text{ } \Omega\text{-cm}^2$  derived from dark J-V measurements for a CdS/CdTe. This contact had a barrier height of 0.3 eV.

The barrier height,  $F_j$ , of the main diode was evaluated at 0K from  $V_{oc}$  versus T, since the contact diode, for a CdTe thickness of  $4 \text{ } \mu\text{m}$ , is in the dark:

$$V_{oc} = (A_j kT / q) \text{Ln} \frac{J_{sc}}{J_{00j}} e^{-\frac{F_j}{A_j kT}} \quad (7)$$

$$V_{oc} = F_j + (A_j kT / q) \text{Ln} \frac{J_{sc}}{J_{00j}} \quad (8)$$

The main junction barrier height was found to be  $\sim 1.4 \text{ eV}$  (Figure 6). The linear behavior over this temperature range demonstrates that the  $J = 0$  bias point of the entire device is not affected by the contact.

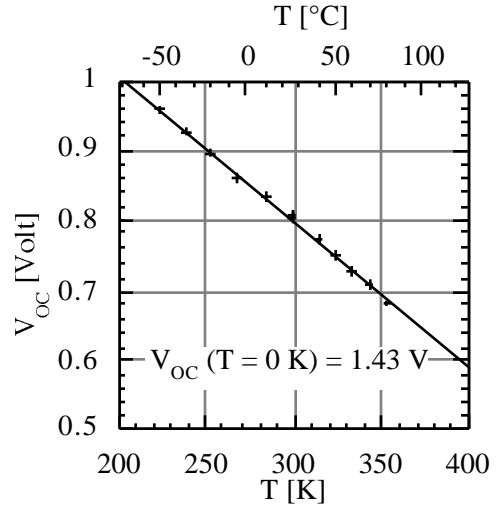
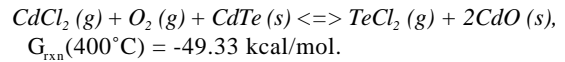


**Figure 6:**  $V_{oc}$  as a function of temperature for a CdS/CdTe device under AM1.5G illumination.

#### 4. CdTe CONTACT SURFACE ANALYSIS

In previous work, we speculated that the chemical process used to prepare the CdTe for application of a current-carrying conductor produced copper tellurides [2]. This has now been confirmed by direct detection of  $\text{Cu}_2\text{Te}$  and  $\text{CuTe}$  phases with glancing incidence x-ray diffraction. The correlation of the glancing incidence x-ray diffraction surface analysis with reaction products expected based on chemical free-energy calculations are described below. During  $\text{CdCl}_2\text{:O}_2$  vapor heat treatment, CdTe reacts with  $\text{CdCl}_2$  and  $\text{O}_2$  resulting in production of CdO on the surface of the CdTe grains according to the reaction:

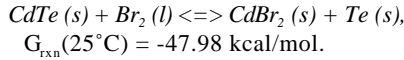
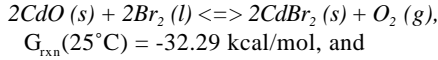


This system leads to the Guldberg and Waage expression of overall chemical equilibrium,

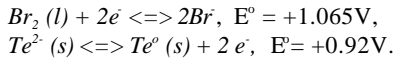
$$K_1 = \frac{[\text{TeCl}_2][\text{CdO}]^2}{[\text{CdCl}_2][\text{O}_2][\text{CdTe}]},$$

in which the quantity of CdO obtained will vary as the square root of  $O_2$  concentration. It is necessary to remove the surface CdO to allow delivery of dopant to the near-surface CdTe and to facilitate formation of a low resistance contact. The CdO is removed by reaction with bromine, which also liberates free Te.

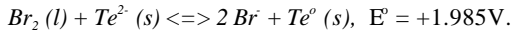
Reaction of CdTe and CdO in  $Br_2:CH_3OH$  are shown to be thermodynamically favored according to:



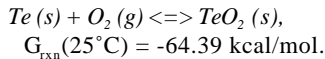
The product  $CdBr_2$  is soluble in methanol and water and is removed from the surface by agitation and rinsing. The reaction to form elemental Te from lattice-bound  $Te^{2-}$  is further described by the room temperature half-cell reactions at the surface:



Adding these reactions and potentials, the highly favored overall reaction is expected:

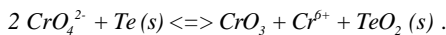


X-ray photoemission spectroscopic (XPS) analysis by Danaher, et. al. [6] on single crystal CdTe reacted in 0.01% (vol)  $Br_2:CH_3OH$  showed Cd-depletion at the surface, extending 3 nm into the surface. They determined an oxidation rate of free Te to be 0.02 nm/minute, according to the favored reaction:

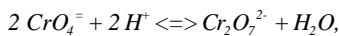


The thin Te coating produced by etching in  $Br_2:CH_3OH$  is not extensive and oxidizes rapidly, diminishing the benefits for doping or contacting; the bromine step is therefore primarily used to eliminate CdO.

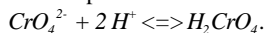
The reaction of CdTe in aqueous  $K_2CrO_4$  produces  $TeO_2$  according to:



The addition of protons to the solution by addition of acid complicates the ionic makeup of the solution. At low pH, the primary effect is the reduction of the chromate ion to dichromate:

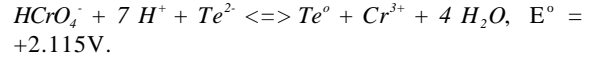
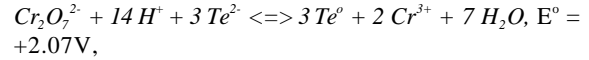


and the production of chromic acid:



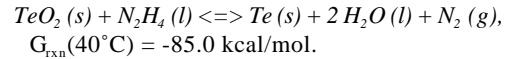
Elemental Te is readily liberated from the CdTe lattice by electrolytic reaction with the chromate or

hypochromous ion. The overall favored reactions and room temperature potentials are:



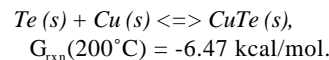
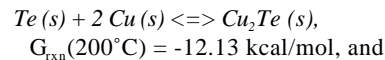
XPS and studies by Danaher, et al. [6] on single crystal CdTe reacted in aqueous  $K_2CrO_4$  and in  $K_2Cr_2O_7:H_2SO_4$  solution confirmed this chemistry, indicating Cd-depleted surface in all cases, with  $TeO_2$  on the surface reacted with aqueous  $K_2CrO_4$  and elemental Te on the surface reacted with 1:1  $K_2Cr_2O_7:H_2SO_4$ . Mixed  $Te:TeO_2$  was obtained on samples reacted with lower acid concentrations. Secondary ion mass spectroscopic depth profiles of reacted CdTe/CdS/ITO films further indicated that Cr penetrated the CdTe film but did not accumulate within the CdS/ITO films [6].

As a final step in producing a Te-enriched surface, reaction in hydrazine solution is carried out. Reactions with  $TeO_2$  powder and 98:2  $N_2H_4:H_2O$  solution at 25-40°C released significant quantities of gas and changed the solution color from clear to faint purple. Similar results were obtained when etching CdTe films after reaction with  $K_2Cr_2O_7:H_2SO_4$ . These observations are consistent with reduction of  $TeO_2$ :



Direct reaction of CdTe with  $N_2H_4$  to produce either elemental Cd or Te is not thermodynamically favored. Glancing incidence x-ray diffraction measurements of CdTe/CdS/ITO thin films confirm the formation of elemental Te after the entire reaction process as shown in Figure 7 (bottom).

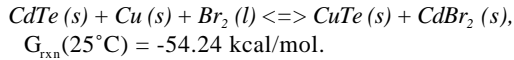
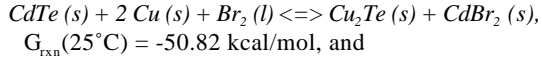
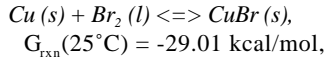
Thus, reaction in acidic dichromate solution liberates additional Te but also forms  $TeO_2$ , depending on the solution pH. Reaction in hydrazine reduces  $TeO_2$  to Te. Deposition and *in situ* heat treatment of this surface with elemental Cu diffuses some Cu into CdTe and leads to production of copper tellurides:



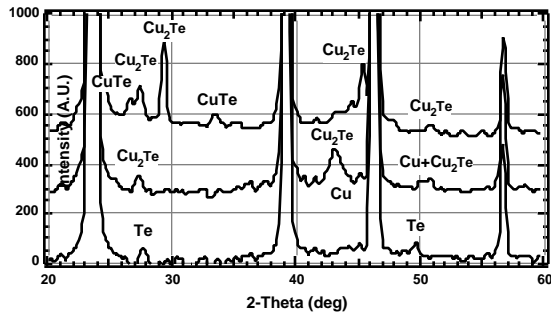
The equilibrium T-x phase diagram for the Cu-Te system shows the possible phases obtained over the full range of relative quantities of Cu and Te [7]. The possible equilibrium phase fields are Cu+  $Cu_2Te$ ,  $Cu_{2-x}Te$ ,  $Cu_{2-x}Te + Cu_3Te_2$ , and  $Cu_3Te_2 + CuTe$ , depending on the relative quantities of Cu and Te. Figure 7 (middle) shows that for excess Cu, the heat treatment produces  $Cu_2Te$ .

Figure 7 (top) shows that reaction with bromine removed excess Cu and resulted in both  $Cu_2Te$  and  $CuTe$

surface phases in an as-yet undetermined configuration. The favored reactions for this are:



In both reactions, the bromide products are soluble in methanol and water and are thus removed by agitation or rinsing. Preliminary experiments show that increasing the proportion of cupric to cuprous tellurides in the final surface increases the non-ohmic contact behavior.



**Figure 7:** Glancing incidence x-ray diffraction patterns of the CdTe surface after three contact treatment steps: (BOTTOM) after hydrazine reaction; (MIDDLE) after Cu deposition and vacuum heat treatment; and (TOP) after bromine reaction.

## 5. SUMMARY

CdS/CdTe solar cells have been analyzed to model the behavior of the CdS/CdTe junction and CdTe contact. The analysis was applied to devices fabricated by physical vapor deposition with carbon contacts and

showed that the main junction and contact are electrically separate with barrier heights of 1.4 and 0.3 eV, respectively. The contact barrier height is attributable to a junction between CdTe and copper tellurides detected at the contact surface. It is expected that this information, coupled with further characterization of the contact region, will lead to improvements in contact performance as well as a better understanding of contact behavior under different thermal, electrical, and illumination stresses.

**Acknowledgments:** The authors acknowledge the contributions of Zhao-Hui Yang, Shannon Fields, Johnny Yu, and Robert W. Birkmire in carrying out this work. This research is supported by a grant from the National Renewable Energy Laboratory, XAK-7-17609-01.

## REFERENCES

- [1] Bulent M Basol, *Int. J. Solar Energy*, **2** (1992) 25.
- [2] B. E. McCandless, Y. Qu, and R. W. Birkmire, *Proceedings 1st World Conference on Photovoltaic Energy Conversion* (1994) 107.
- [3] B. E. McCandless, R. W. Birkmire, D. G. Jensen, J. E. Phillips, and I. Youm, *Proceedings 14th NREL PV Program Review Meeting*, AIP Publications (1996) 647.
- [4] P.V. Meyers and J. E. Phillips, *Proceedings 25th IEEE PVSC* (1996) 789.
- [5] B. E. McCandless, H. Hichri, G. Hanket, and R. W. Birkmire, *Proceedings 25th IEEE PVSC* (1996) 781.
- [6] W. J. Danaher, L. E. Lyons, M. Marychurch, and G. C. Morris, "Chemical Etching of Crystal and Thin Film Cadmium Telluride", *Applied Surface Science*, **27** (1986) 338.
- [7] T. B. Massalski, *Binary Alloy Phase Diagrams*, 2nd Edition, ASM Int: Materials Park, OH (1990).